$\bar{p}p$ annihilation into $\bar{D}D$ meson pair within an effective Lagrangian model

R. Shyam[1,2] and H. Lenske[2]

[1]*Saha Institute of Nuclear Physics, 1/AF Bidhan Nagar, Kolkata 700064, India*
[2]*Institut für Theoretische Physik, Universität Gieseen, Heinrich-Buff-Ring 16, D-35392 Giessen, Germany*

(Received 14 September 2015; published 9 February 2016)

We study the charmed meson pair ($\bar{D}^0D^0$ and D^+D^-) production in $\bar{p}p$ annihilation within an effective Lagrangian model that has only the baryon-meson degrees of freedom and involves the physical hadron masses. The reaction amplitudes include terms corresponding to the t-channel Λ_c^+, Σ_c^+, and Σ_c^{++} baryon exchanges and the s-channel excitation, propagation and decay of the $\Psi(3770)$ resonance into the charmed mesons. The initial- and final-state distortion effects have been accounted for by using a simple eikonal approximation-based procedure in the same way as was done in our previous study of the $\bar{p}p \to \bar{\Lambda}_c^-\Lambda_c^+$ reaction within a similar model. The $\bar{D}^0D^0$ production reaction is dominated by the Λ_c^+ baryon exchange process and the corresponding total cross sections are predicted to be in the range of $0.18 - 0.7$ μb for antiproton beam momenta varying between threshold and 20 GeV/c. The $\Psi(3770)$ resonance contributions have a large influence on the differential cross sections of the D^-D^+ production reaction.

DOI: 10.1103/PhysRevD.93.034016

I. INTRODUCTION

The first discovery of a charm-anticharm ($c\bar{c}$) bound state (J/ψ) [1,2] was made more than 30 years ago. Yet a substantial part of the charmonium spectrum is still to be precisely measured. Due to several reasons, charmonium states (and other heavy quarkonium states) have played an important role in our understanding of quantum chromodynamics (QCD), the fundamental theory of the strong interaction. Within the range of momentum exchange in bound $c\bar{c}$ systems, the value of the strong coupling constant α_s is not so large to invalidate the application of the perturbative methods. Thus these states provide a unique laboratory to explore the interplay between perturbative and nonperturbative effects in QCD. The relatively small binding energy of the charmonium as compared to the rest mass of its constituents allows its description by the nonrelativistic approaches that simplify and constrain the analysis of the nonperturbative effects (see, e.g. Ref. [3], for a recent review). These mostly analytical methods are of considerable help in making significant progress in lattice QCD calculations, which have become increasingly more capable of dealing quantitatively with the nonperturbative dynamics in all its aspects (see, e.g., Refs. [4,5]).

Therefore, there is considerable interest in investigations of the production of charmonium states. Experimentally, they have been studied mainly in electron-positron and proton-antiproton annihilation processes. However, there are distinct advantages in producing $c\bar{c}$ states in the latter method where all the three valence quarks in a proton annihilate with their corresponding antiquark partners in an antiproton. This does not set any constraint on the quantum numbers of the final states enabling one to reach all the charmonium states by the direct formation. On the other hand, in electron-positron annihilation, the direct creation of final charmonium states is constrained to the quantum numbers of the photon ($J^{PC} = 1^{--}$). Other states can be reached only indirectly by other mechanisms.

The $\bar{P}ANDA$ ("antiproton annihilation at Darmstadt") experiment will use the antiproton beam from the Facility for Antiproton and Ion Research (FAIR) colliding with an internal proton target and a general purpose spectrometer to carry out a rich program on the charmonium production in proton-antiproton annihilation. The entire energy region below and above the open charm threshold will be explored in these studies. Charmonium states above the open charm threshold will generally be identified by means of their decays to $\bar{D}D$ [6–8], unless this is forbidden by some conservation rule.

The reliable estimation of the rates of $\bar{p}p \to \bar{D}^0D^0$ and $\bar{p}p \to D^-D^+$ reactions (to be together referred to as the $\bar{p}p \to \bar{D}D$ reaction) at the $\bar{P}ANDA$ energies is required for the accurate detection of the charmonium states above the $\bar{D}D$ threshold. In addition, it is also important for other studies such as open charm spectroscopy, the search for charmed hybrids decaying to $\bar{D}D$, the investigation of the rare decays and of the charge-conjugation-parity violation in the D-meson sector. All these topics are the major components of the $\bar{P}ANDA$ physics program [6]. The accurate knowledge of these reactions is also the primary requirement for investigating the creation of the exotic flavored nuclear systems like charmed hypernuclei [9–11] and charmed D-mesic nuclei [12–14].

The cross sections of the $\bar{p}p \to \bar{D}D$ reaction have been calculated by several authors employing a variety of models. In Ref. [15], a nonperturbative approach has been used, which is based on the $1/N$ expansion in QCD, Regge asymptotics for hadron amplitudes, and a string model. Similar types of models were used in the

calculations reported in Refs. [16,17]. In Ref. [18], the $\bar{p}p \to \bar{D}^0 D^0$ reaction has been described within a double handbag model where the amplitude is calculated by convolutions of hard subprocess kernels (representing the transition $u\bar{u} \to c\bar{c}$) and the generalized parton distributions, which represent the soft nonperturbative physics. This approach was earlier used in Ref. [19] to describe the production of $\bar{\Lambda}_c^- \Lambda_c^+$ in $\bar{p}p$ annihilation and it resembles the quark-diquark picture that was employed by this group to make predictions for the cross sections of the $D^- D^+$ reaction in Ref. [20].

Recently the production of $\bar{D}D$ in antiproton-proton annihilation has been studied within the Jülich meson-exchange model in Ref. [21]. This approach was employed earlier to investigate the $\bar{p}p \to \bar{\Lambda}\Lambda$ [22,23] and $\bar{p}p \to \bar{\Lambda}_c^- \Lambda_c^+$ [24,25] reactions. In this model, these processes are considered within a coupled-channels framework, where the initial- and final-state interactions are taken into account in a rigorous way. The reactions proceed via the exchange of appropriate mesons between $\bar{p}$ and p leading to the final baryon-antibaryon states.

Apart from Ref. [18], where the calculated total cross section ($\sigma_{\rm tot}$) for the $\bar{p}p \to \bar{D}^0 D^0$ reaction was reported to be below 10 nb, in the majority of the calculations, the magnitudes of the $\sigma_{\rm tot}$ for this reaction lie in the range of 10–100 nb. However, the predictions of various models differ significantly for the cross section of the $\bar{p}p \to D^- D^+$ reaction.

In this paper, we present the results of our investigations for the cross sections of $\bar{p}p \to \bar{D}^0 D^0$, and $\bar{p}p \to D^- D^+$ reactions within a single-channel effective Lagrangian model (see, e.g., Refs. [26–28]), where these reactions are described as a sum of the t-channel Λ_c^+, Σ_c^+, Σ_c^{++} baryon exchange diagrams [see, Figs. 1(a) and 1(b)] and the s-channel excitation, propagation and decay into the $D\bar{D}$ channel of the $\Psi(3770)$ resonance (presented diagrammatically in Fig. 2). The t-channel part of the model is similar to that used in our previous calculation [29] of the $\bar{p}p \to \bar{\Lambda}_c^- \Lambda_c^+$ reaction that proceeds via the t-channel D^0 and D^{*0} meson-exchange processes.

In the next section, we present our formalism. The results and discussions of our work are given in Sec. III. Finally, the summary and the conclusions of this study are presented in Sec. IV.

II. FORMALISM

The exchanges of both Λ_c^+ and Σ_c^+ baryons contribute to the t-channel amplitude of the $\bar{p} + p \to \bar{D}^0 + D^0$ reaction. However, the process $\bar{p} + p \to D^- + D^+$ is mediated only by the exchange of the Σ_c^{++} baryon in the t channel. On the other hand, the s-channel excitation, propagation and subsequent decay of the intermediate resonance state $\psi(3770)$ contribute to both these reactions.

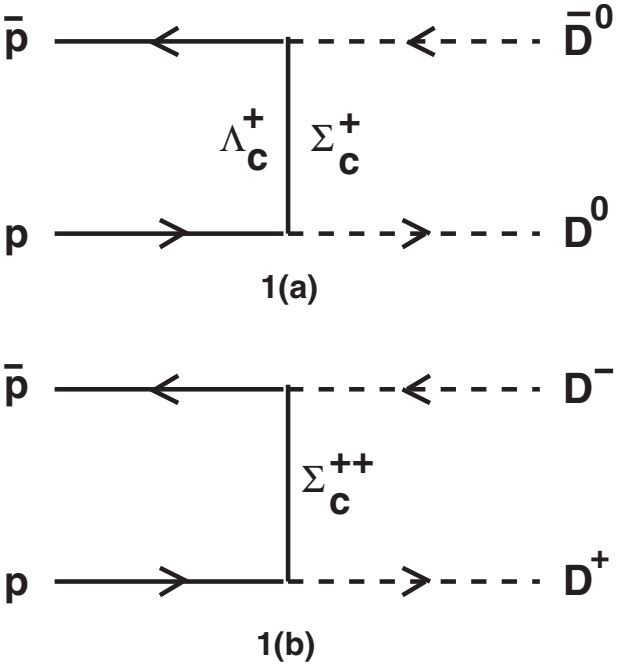

FIG. 1. Graphical representation of the model used to describe the $\bar{p} + p \to \bar{D}^0 + D^0$ (a) and $\bar{p} + p \to D^- + D^+$ (b) reactions via t-channel exchange of charmed baryons. In (a) Λ_c^+ and Σ_c^+ in the intermediate line represent the exchanges of Λ_c^+ and Σ_c^+ baryons, respectively while in (b) Σ_c^{++} represents the exchange of Σ_c^{++} baryon.

To evaluate amplitudes for the processes shown in Figs. 1 and 2, we have used the effective Lagrangians at the charm baryon-meson-nucleon vertices, which are taken from Refs. [29–33]. For the vertices involved in the t-channel diagrams we have

$$\mathcal{L}_{NBD} = i g_{NBD} \bar{\psi}_N i\gamma^5 \phi_D \psi_B + \text{H.c.}, \tag{1}$$

where ψ_N and ψ_B are the nucleon (antinucleon) and charmed baryon fields, respectively, and ϕ_D is the D-meson field. g_{NBD} in Eq. (1) represents the vertex coupling constant.

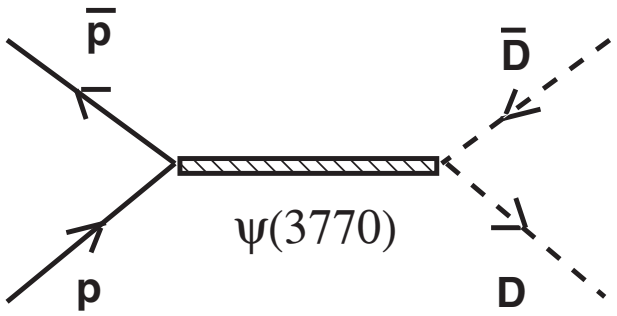

FIG. 2. The Feynman diagram to describe the $\bar{p} + p \to \bar{D} + D$ reaction via s-channel excitation, propagation and decay of the $\Psi(3770)$ resonance.

The amplitude of the diagrams given in Figs. 1(a) and 1(b) is given by

$$A(B) = i\frac{g_{NBD}^2}{q^2-(m_B-i\Gamma_B/2)^2}\bar{\psi}_{\bar{p}}(k_{\bar{p}}) \times \gamma^5(\gamma_\mu q^\mu + m_B)\gamma^5\psi_p(k_p), \quad (2)$$

where B represents the exchanged charmed baryon. q, m_B and Γ_B are the momentum, mass and the width of the exchanged charmed baryon, respectively. The term that contains these quantities comes from the propagator of these baryons. The widths of the charmed baryons are taken from the latest Particle Data Group estimates [34]. The coupling constants g_{NBD} are adopted from Refs. [30,31], as $g_{N\Lambda_c^+D} = 13.50$, $g_{N\Sigma_c^+D} = 2.69$ and $g_{N\Sigma_c^{++}D} = 2.69$. From these values it is expected that Λ_c^+ will dominate the t-channel production amplitudes.

The off-shell behavior of the vertices is regulated by a monopole form factor (see, e.g., Refs. [26,27])

$$F_i(q_{B_i}) = \frac{\lambda_i^2 - m_{B_i}^2}{\lambda_i^2 - q_{B_i}^2}, \quad (3)$$

where q_{B_i} is the momentum of the ith exchanged baryon with mass m_{B_i}. λ_i is the corresponding cutoff parameter, which governs the range of suppression of the contributions of high momenta carried out via the form factor. We chose a value of 3.0 GeV for λ_i at all the vertices. The same λ_i was also used in the monopole form factor employed in the study of the reaction $\bar{p}p \to \bar{\Lambda}_c^- \Lambda_c^+$ in Ref. [29] within a similar model. It may be mentioned here that in the Jülich meson-exchange model calculations of the reaction $\bar{p} + p \to \bar{D} + D$ presented in Ref. [21], a form factor of the following type has been used:

$$F_i(q_{B_i}) = \left[\frac{(\lambda_i)^4}{(\lambda_i)^4 + (q_i^2 - m_{B_i}^2)^2}\right] \quad (4)$$

with a λ_i of 3.5 GeV. This form factor gives more weight to the lower momentum transfers. As discussed below we use this type of form factor at the resonance production and decay vertices.

In order to evaluate the diagram of Fig. 2, the effective Lagrangians are required at $\Psi\bar{p}p$ and $\Psi\bar{D}D$ vertices, which are written as

$$\mathcal{L}_\mu^{\Psi\bar{p}p} = g_{\Psi\bar{p}p}\left[\bar{\psi}_{\bar{p}}\left(\gamma_\mu + \frac{\kappa_\Psi}{2M}\sigma_{\mu\nu}\partial^\nu\theta_\Psi^\mu\right)\psi_p\right], \quad (5)$$

and

$$\mathcal{L}_{\Psi\bar{D}D} = g_{\Psi\bar{D}D}(\Phi_{\bar{D}}\partial_\mu\Phi_D)\theta_\Psi^\mu. \quad (6)$$

In Eq. (5) M represents the nucleon mass and θ_Ψ^μ is the Ψ resonance field. $g_{\Psi\bar{p}p}$ and κ_Ψ are the coupling constants at the $\Psi\bar{p}p$ vertex. Similarly, in Eq. (6) $g_{\Psi\bar{D}D}$ is the coupling constant at the $\Psi\bar{D}D$ vertex and $\Phi_{\bar{D}}$ and Φ_D represent the $\bar{D}$ and D charmed meson fields. The values of the coupling constants $g_{\Psi\bar{D}^0D^0}$, $g_{\Psi D^-D^+}$ and $g_{\Psi\bar{p}p}$ have been determined from the branching ratios for the decay of the $\Psi(3770)$ resonance to the relevant channels as given in Refs. [35] and [36]. We take $g_{\Psi\bar{D}^0D^0} = 17.90$ (see also Ref. [37]), $g_{\Psi D^-D^+} = 14.10$ and $g_{\Psi\bar{p}p} = 5.12\times10^{-3}$. The value of κ_Ψ is fixed by fitting the cross sections of the $\bar{p} + p \to \Psi(3770) \to \bar{D}^0D^0$ calculated within the effective Lagrangian model to that obtained within a semiclassical resonance production and decay model where experimental widths for the decay processes $\Psi \to \bar{p}p$ and $\Psi \to \bar{D}D$ are used. This is discussed in the next section.

The amplitude of the process $\bar{p} + p \to \Psi(3770) \to \bar{D}D$ (Fig. 2) is written as

$$A(\Psi) = -g_{\Psi\bar{p}p}g_{\Psi\bar{D}D}\frac{1}{s_{\rm inv}-(m_\Psi - i\Gamma_\Psi/2)^2} \times \left[\psi_{\bar{p}}\left(\gamma_\mu + \frac{i\kappa_\Psi}{2M}\sigma_{\mu\nu}q^\nu\right)\psi_p\right](k_{\bar{D}} - k_D)^\mu, \quad (7)$$

where $k_{\bar{D}}$ and k_D are the momenta associated with the final-state $\bar{D}$ and D mesons, respectively, and $s_{\rm inv}$ is the square of the invariant mass associated with the Ψ resonance. It may be mentioned that the denominator of the Ψ propagator leads to a cross section that has a pole in the vicinity of the physical mass value (m_Ψ) of the Ψ resonance, which is taken to be 3773.15 MeV. The total width (Γ_Ψ) of this resonance is 27.2 MeV [34]. A similar approach for the denominator of the Ψ propagator has also been adopted in Refs. [38–40]. This procedure is inspired by the extreme vector-meson dominance hypothesis where contributions of the vector-meson resonance are included in the vicinity of the relevant kinematical regime and in the far off-shell vector-meson kinematical regions it is considered as background that is generally quite weak.

In order to account for the off-shell effects due to the internal structure of the intermediate charmonium states, we introduce vertex form factors for the Ψ resonance. In our calculations the shapes of these form factors are given by Eq. (4) with cutoff parameters

$$\lambda_\Psi = m_\Psi + \alpha\lambda_{\rm QCD}, \quad (8)$$

where $\lambda_{\rm QCD} = 240$ MeV, and α is an adjustable parameter. We have used $\alpha = 7.5$ for amplitudes involving the $\Psi(3770)$ resonance.

A widely used approach is to parametrize the total cross section for the process $\bar{p}p \to \psi(3770) \to \bar{D}D$ in a Breit-Wigner form (see, e.g. Refs. [35,41,42])

$$\sigma_{\bar{p}p\to\psi(3770)\to\bar{D}D} = \frac{2J_\Psi+1}{(2j_{\bar{p}}+1)(2j_p+1)}\frac{4\pi}{q^2_{\bar{p}p}} \times \frac{s_{\rm inv}\Gamma_{\Psi(3770)\to\bar{p}p}\Gamma_{\Psi(3770)\to\bar{D}D}}{(s_{\rm inv}-M^2_\psi)^2+s_{\rm inv}\Gamma^2_{\rm tot}}, \quad (9)$$

where J_Ψ is the spin of the resonance and $q_{\bar{p}p}$ is the momentum in the $\bar{p}p$ channel. $\Gamma_{\Psi(3770)\to\bar{p}p}$ is the partial width for the production process $\bar{p}p\to\Psi$ and $\Gamma_{\Psi(3770)\to\bar{D}D}$ is the partial width for the $\Psi\to\bar{D}D$ decay. $\Gamma_{\rm tot}$ is the total width of the Ψ resonance. Attempting to account for the possible self-energy contributions to the formation and decay of the resonance, some authors (see, e.g., Ref. [42]) have introduced an energy dependence to the width $\Gamma_{\Psi(3770)\to\bar{D}D}$ adopted from Ref. [43]. The ansatz for this energy dependence involves the range of $\bar{D}D$ interactions, which is treated as a free fitting parameter. For the sake of simplicity and in order to keep the number of adjustable parameters as small as possible, here we refrain from such a more elaborate approach. We use a constant width, which is a good approximation in view of the very narrow line width of the $\Psi(3770)$ resonance. In fact, close to the resonance pole, the expression given by Eq. (9) is indeed a very good approximation of the exact result [40].

In our numerical calculations, we have used for $\Gamma_{\Psi(3770)\to\bar{D}D}$ the values extracted from the branching ratios of this decay as given in the latest compilation of the Particle Data Group (PDG) [34]. The width $\Gamma_{\Psi(3770)}\to\bar{p}p$ is obtained from the branching fraction $B_{\Psi\to\bar{p}p}=7.1^{+8.6}_{-2.9}\times10^{-6}$ as reported in Ref. [36]. We have taken the width corresponding to the upper limit of $B_{\Psi\to\bar{p}p}$, which was also employed in the determination of the coupling constant $g_{\Psi\bar{p}p}$ used in Eq. (7).

From the studies of the $\bar{\Lambda}^-_c\Lambda^+_c$ production [24,29], it is well known that the magnitudes of the cross sections depend very sensitively on the initial-state distortion effects. In fact, the $\bar{p}p$ annihilation channel is almost as strong as the elastic scattering channel. This large depletion of the flux can be accounted for by introducing absorptive potentials that are used in optical models or in coupled-channels approaches [22–24,44,45]. In this work, instead of employing such a detailed treatment, we use a procedure that was originated by Sopkovich [46] and was employed in Ref. [29] for describing the $\bar{p}p\to\bar{\Lambda}^-_c\Lambda^+_c$ reaction. In this method, the transition amplitude for the reaction $\bar{p}p\to\bar{D}D$ with distortion effects is written as

$$T^{\bar{p}p\to\bar{D}D} = \sqrt{\Omega^{\bar{p}p}}T^{\bar{p}p\to\bar{D}D}_{\rm Born}\sqrt{\Omega^{\bar{D}D}} \quad (10)$$

where $T^{\bar{p}p\to\bar{D}D}_{\rm Born}$ is the transition matrix calculated within the plane-wave approximation and $\Omega^{\bar{p}p}$ and the $\Omega^{\bar{D}D}$ are the operators describing the initial- and final-state elastic interactions, respectively.

For the present purpose, we neglect the real part of the baryon-antibaryon interaction. Considering the $\bar{p}p$ initial-state interaction (ISI), we describe the strong absorption by an imaginary potential of Gaussian shape with range parameter μ and strength V_0. By using the eikonal approximation, the corresponding attenuation integral can be evaluated in a closed form. Similar to Refs. [46,47], we obtain for $\Omega^{\bar{p}p}$

$$\Omega^{\bar{p}p} = \exp\left[\frac{-\sqrt{\pi}EV_0}{\mu k}\exp(-\mu^2b^2)\right], \quad (11)$$

where b is the impact parameter of the $\bar{p}p$ collision. E and k are the center-of-mass energy and the momentum of the particular channel, respectively. In our numerical calculations, we have used the same values for the parameters V_0, μ and b as in Ref. [29]. It may be noted that with these parameters we were able to get cross sections for the $\bar{p}p\to\bar{\Lambda}\Lambda$ strangeness production reaction in close agreement with the corresponding experimental data. Furthermore, our cross sections for the $\bar{p}p\to\bar{\Lambda}^-_c\Lambda^+_c$ reaction were similar in magnitude to those reported in a coupled-channels meson-exchange model calculation [24].

In the case of the $\bar{p}p\to\bar{\Lambda}^-_c\Lambda^+_c$ reaction, it has been shown in Ref. [24] that, because of the strong absorption in the initial channel, the production cross sections were rather insensitive to the final-state interaction (FSI) between $\bar{\Lambda}^-_c$ and Λ^+_c. In Ref. [21], the effects of the $\bar{D}D$ FSI were investigated by approximately extending in the charmed meson sector the $\pi\pi\to\bar{K}K$ model of the Jülich group [48]. However, these calculations have sizable uncertainties and even then the effect of FSI is not big. In our procedure, unlike the $\bar{p}p$ ISI, it is not possible to put any constraint, experimental or otherwise, on the choice of the $\bar{D}D$ FSI distortion parameters. Therefore, in order to keep the number of free parameters small, like our study on $\bar{\Lambda}^-_c\Lambda^+_c$ production, we concentrate only on the initial-state interaction in this study. It should be mentioned that also in calculations reported in Refs. [15–17] the meson-meson FSI effects were not considered.

The distortion effects could lead to the reduction of the undistorted cross sections by several orders of magnitude depending upon the values of the parameters V_0, μ and b. In Fig. 3, we have shown $\Omega_{\bar{p}p}$ as function of the beam momentum $p_{\bar{p}}$ with the values of parameters μ, V_0 and b being 0.3369 GeV, 0.8965 GeV and 0.3270 GeV^{-1}, respectively. We see that $\Omega_{\bar{p}p}$ increases gradually as $p_{\bar{p}}$ goes beyond the threshold and becomes almost constant at higher values of $p_{\bar{p}}$—in this region the values of E and k are roughly equal. With this $\Omega_{\bar{p}p}$, the undistorted cross sections would dampen by almost 2 orders of magnitude. As far as dependencies on the parameters are concerned, increasing V_0 obviously increases the damping, while decreasing μ has the same effect.

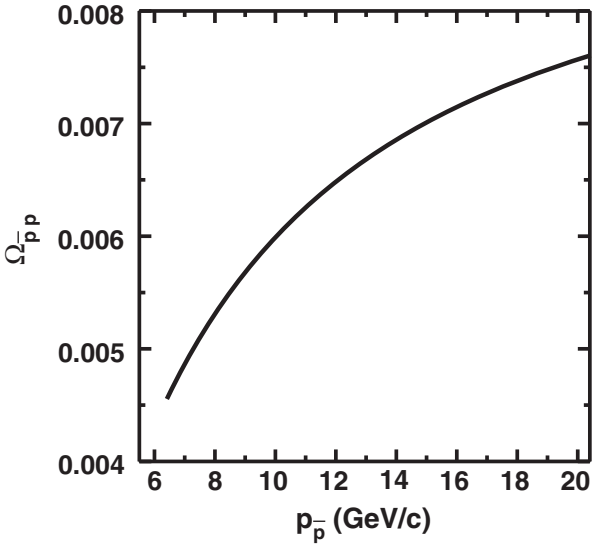

FIG. 3. The distortion factor $\Omega_{\bar{p}p}$ [defined by Eq. (11)] as a function of the antiproton beam momentum. The values of the parameters μ, V_0 and b were taken to be 0.3369 GeV, 0.8965 GeV and 0.3270 GeV^{-1}, respectively, which are the same as those used in Ref. [29].

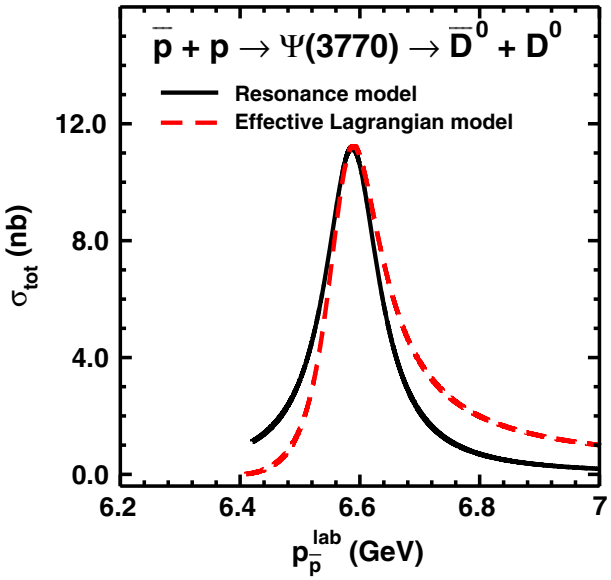

FIG. 4. Total cross section for the $\bar{p}p \rightarrow \Psi(3770) \rightarrow \bar{D}^0 D^0$ reaction as a function of the antiproton beam momentum. The solid line represents the cross sections calculated within the resonance production and decay model [Eq. (9)], while the dashed line shows the effective Lagrangian model cross sections [obtained with the amplitude given by Eq. (7)].

III. RESULTS AND DISCUSSIONS

One can estimate the total cross sections for the $\bar{p}p \rightarrow \bar{D}^0 D^0$ and $\bar{p}p \rightarrow D^- D^+$ reactions around the $\Psi(3770)$ peak with the help of Eq. (9). With the values of various widths extracted from the experimental data as specified in the last section, the total cross sections calculated by Eq. (9) can indeed be used to fix some of the parameters of the effective Lagrangian model (ELM). We deduce the parameter κ_Ψ in Eq. (5) by comparing the total cross section for e.g., the $\bar{p}p \rightarrow \psi(3770) \rightarrow \bar{D}^0 D^0$ reaction calculated within the ELM [by using the amplitude given by Eq. (7)] with that obtained by Eq. (9). In the ELM calculations the $\bar{p}p$ ISI has been included. In Fig. 3, we show this comparison where the value of κ_Ψ is taken to be 6.0.

In Fig. 4, we see that the peak of the ELM cross sections coincides with that of the resonance model. Also, in the vicinity of the resonance peak the two models predict the same magnitudes of the cross sections and the same line shapes. The value of this cross section is about 12 nb at the peak position, which is close to the lower limit of $\sigma_{\rm tot}$ predicted in Ref. [40].

In Figs. 5(a) and 5(b) we present the results for the total cross sections of $\bar{p}p \rightarrow \bar{D}^0 D^0$ and $\bar{p}p \rightarrow D^- D^+$ reactions, respectively, for antiproton beam momenta ($p_{\bar{p}}^{\rm lab}$) in the region of 6.4–6.8 GeV/c, where the $\Psi(3770)$ resonance is expected to show its impact. In these figures, solid lines represent the cross sections where the amplitudes of the t-channel baryon exchanges and the s-channel $\Psi(3770)$ production and decay are coherently added, while the dashed lines include only the t-channel baryon exchange contributions. We see in Fig. 5(a) that for the $\bar{p}p \rightarrow \bar{D}^0 D^0$ reaction the cross sections corresponding to the t-channel baryon exchange processes are fairly large (∼300 nb) in the resonance peak (RP) region, so the inclusion of the $\Psi(3770)$ resonance contributions does not make any dramatic effect. It just produces a small kink in the cross section around the RP momentum. This is in contrast to the results of Ref. [40], where the $\Psi(3770)$ resonance led to an enhancement of almost a factor of 2 in the cross sections of the $\bar{p}p \rightarrow \bar{D}^0 D^0$ reaction around the RP region. The reasons for this difference can be attributed to two facts. First, our t-channel baryon exchange cross sections are larger than those of Ref. [40] (about 300 nb as compared to only about 40 nb) in the RP region, and second, our cross sections for the $\Psi(3770)$ resonance excitation are smaller than those of Ref. [40] in this region.

On the other hand, in our study the effect of the $\Psi(3770)$ resonance is quite prominent for the $\bar{p}p \rightarrow D^- D^+$ reaction as can be seen in Fig. 5(b). In our model, the t-channel baryon exchange contributions to the cross sections of this reaction are strongly suppressed. The reason for this is that only the Σ^{++} exchange mediates the t-channel amplitude in this case, which becomes very small because of the much smaller coupling constant and somewhat larger mass of the exchanged baryon. The ratio of the absolute magnitudes of the $\bar{p}p \rightarrow \bar{D}^0 D^0$ and $\bar{p}p \rightarrow D^- D^+$ reactions is roughly proportional to $(g_{N\Lambda_c^+ D}/g_{N\Sigma_c^{++} D})^4$, which leads to a reduction in the $D^- D^+$ production cross section over that of $\bar{D}^0 D^0$ by nearly a factor of 650.

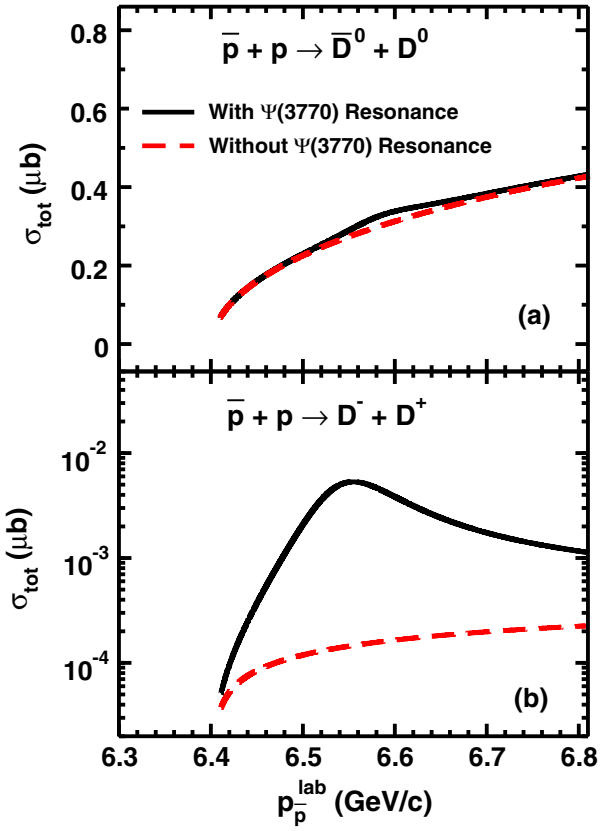

FIG. 5. (a) Total cross section for the $\bar{p}p \to \bar{D}^0 D^0$ reaction as a function of the antiproton beam momentum. The solid and dashed lines represent the cross sections obtained by the coherent sum of the t-channel baryonic exchange and the s-channel $\Psi(3770)$ resonance excitation amplitudes, and by including the t-channel baryon exchange contributions only in the amplitude, respectively. (b) The same for the $\bar{p}p \to D^- D^+$ reaction as a function of the antiproton beam momentum. The full and dashed lines have the same meaning as in (a).

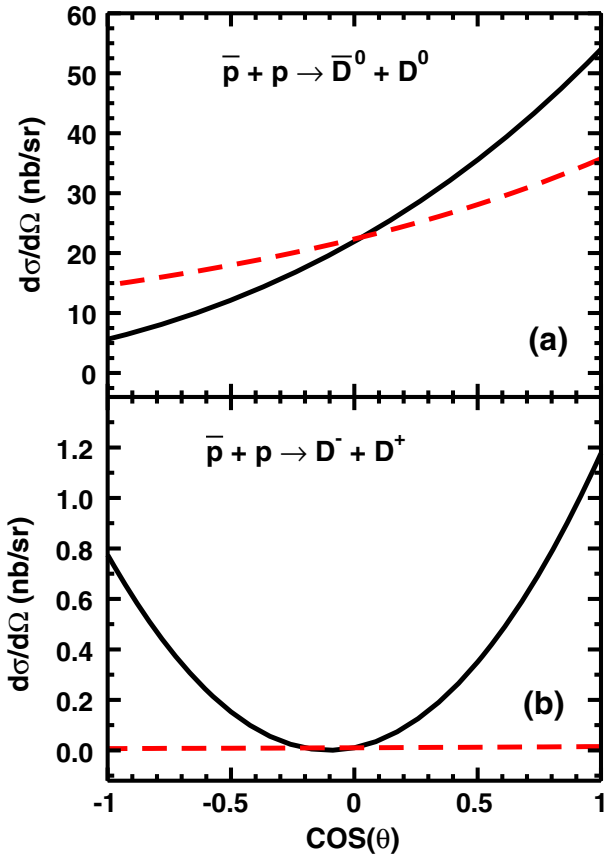

FIG. 6. (a) Differential cross section for the $\bar{p}p \to \bar{D}^0 D^0$ reaction at the antiproton beam momentum of 6.57 GeV/c. The solid and dashed lines have the same meanings as those in Fig. 5. (b) The same as in (a) but for the $\bar{p}p \to D^- D^+$ reaction.

It should, however, be mentioned here that in the consideration of the ISI within the distorted-wave Born approximation approach (Ref. [21]), two-step transitions of the form $\bar{p}p \to \bar{n}n \to D^- D^+$, are generated. Because the Λ_C^+ exchange can contribute to the $\bar{n}n \to D^- D^+$ transition potential, this exchange is no longer absent. Therefore, these two-step mechanisms can enhance the $D^- D^+$ production cross sections. Indeed, in Refs. [21,40] the cross sections for $D^- D^+$ production are even larger than those of the $\bar{D}^0 D^0$ production. On the other hand, such two-step mechanisms are out of the scope of our as well as of Regge model [15–17] calculations. Therefore, in studies within these models the cross sections of the $\bar{p}p \to D^- D^+$ reaction are suppressed as compared to those of the $\bar{p}p \to \bar{D}^0 D^0$ reaction.

In Figs. 6(a) and 6(b) we show the differential cross sections (DCS) for $\bar{p}p \to \bar{D}^0 D^0$ and $\bar{p}p \to D^- D^+$ reactions, respectively, at the beam momentum of 6.57 GeV/c, which corresponds to the Ψ resonance invariant mass $(\sqrt{s_{\rm inv}}) = 3770.24$ MeV. Therefore, these cross sections represent the angular distributions of the produced charmed mesons at practically the resonance peak. In Fig. 6(a), we note that the inclusion of the $\Psi(3770)$ resonance alters significantly the cross section obtained with only the t-channel baryon exchange term (dashed line). Strong interference effects of various amplitudes are evident. At the backward angles, the t-channel baryon exchange and s-channel $\Psi(3770)$ amplitudes interfere destructively while at forward angles this interference is constructive leading to the strong forward peaking of the angular distribution. Because of this interference effect, the DCS do not exhibit the type of shape that is expected from a pure p-wave resonance dominated amplitude.

On the other hand, in Fig. 6(b), the differential cross section obtained by adding the s-channel $\Psi(3770)$ terms to the t-channel baryon exchange amplitudes shows a dominant p-wave type of angular distribution. This is due to the fact that contributions of the $\psi(3770)$ resonance term are significantly stronger than those of the t-channel baryon exchange term in this case. This was apparent already in Fig. 5(b). However, even though the t-channel baryon exchange amplitudes are relatively quite small, they do

introduce some distortion to the angular distribution of the D mesons arising from the decay of the $\Psi(3770)$ resonance through the interference terms. This is evident from the asymmetry of the $\cos(\theta)$ distribution depicted by the solid curve.

In general, the interference patterns in the differential cross sections depend quite sensitively on the relative magnitudes of the t-channel baryon exchange and s-channel $\Psi(3770)$ amplitudes. Thus, they provide a critical check on the coupling constants that enter into these amplitudes. Therefore, measurements of the differential cross sections of these reactions in future experiments would be useful in fixing these coupling constants.

Next, we discuss the charm meson production in antiproton-proton annihilation at higher beam energies. In Fig. 7, we show the total cross section of the $\bar{p} + p \to \bar{D}^0 D^0$ reaction for antiproton beam momentum varying in the range of threshold to 20 GeV/c. In this figure, the roles of various t-channel baryon exchange and the s-channel $\Psi(3770)$ resonance excitation processes have been investigated. We note that $\sigma_{\rm tot}$ for this case is almost solely governed by the Λ_c-exchange mechanism in the entire range of the antiproton beam momentum. The contributions of Σ_c^+-exchange terms are lower by about 3 orders of magnitudes. This can be understood from the approximate proportionality of the ratio of $\sigma_{\rm tot}$ of the two exchange processes to the fourth power of the ratio of the coupling constants of respective vertices involved in the corresponding amplitudes as discussed above. The s-channel $\Psi(3770)$-exchange term contributes negligibly to the $\sigma_{\rm tot}$ of this reaction at higher beam momenta.

We further note in Fig. 7 that the $\sigma_{\rm tot}$ peaks at a $p_{\bar{p}}^{\rm lab}$ of about 9 GeV/c. This is in agreement with the results of the Regge trajectory model calculations of Refs. [16] and [15]. At the beam momentum of interest to the $\bar{P}ANDA$ experiment (15 GeV/c), the total cross section for the $\bar{D}^0 D^0$ production reaction predicted by our model is about 570 nb. This should be compared with the results reported by other authors for this beam momentum. In Refs. [16] and [15] the corresponding cross sections are approximately 100 and 70 nb, respectively, while in Ref. [18] it is less than 10 nb. We recall that in Refs. [16] and [15], the ISI effects were included by following an eikonal-model-based procedure similar to that of our study. Of course, uncertainties in this method can not be ruled out. However, in our calculations, we have taken the same ISI parameters in Eq. (11) as those used in our previous study [29] of the $\bar{p}p \to \bar{\Lambda}_c^- \Lambda_c^+$ reaction within a similar model. These parameters were checked by reproducing the near-threshold cross section predicted within the Jülich meson-exchange model calculations of this reaction reported in Refs. [24,25] where ISI effects have been treated more rigorously within a coupled-channels method.

In Fig. 8, we present the total cross sections for the $\bar{p}p \to D^- D^+$ reaction as a function of the antiproton beam momentum. We see that the $\sigma_{\rm tot}$ of this reaction is strongly suppressed compared to that of Fig. 7. This was seen already in Fig. 5 at near-threshold beam momenta.

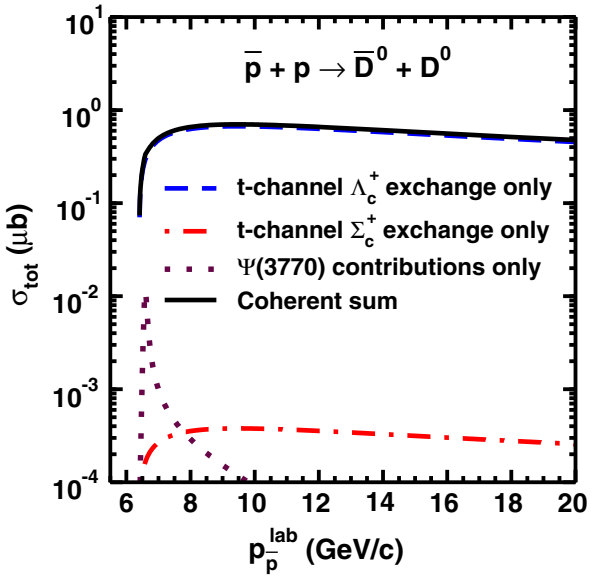

FIG. 7. Total cross section for the $\bar{p}p \to \bar{D}^0 D^0$ reaction as a function of the antiproton beam momentum. The contributions of t-channel Λ_c^+ and Σ_c^+ baryon exchange processes are shown by dashed and dashed-dotted lines, respectively, while the dotted line represents the cross sections of the s-channel $\Psi(3770)$ resonance excitation. The cross sections corresponding to the coherent sum of these amplitudes are shown by the full curve.

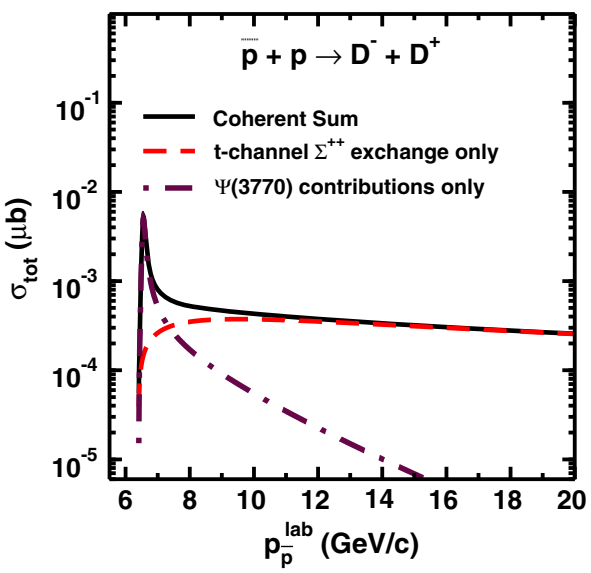

FIG. 8. Total cross section for the $\bar{p}p \to D^- D^+$ reaction as a function of the antiproton beam momentum. The contributions of t-channel Σ_c^{++} baryon exchange and s-channel $\Psi(3770)$ resonance excitation are shown by dashed and dash-dotted lines respectively. The cross sections corresponding to the coherent sum of these terms in the total amplitudes are shown by the full curve.

A similar suppression of D^-D^+ cross sections relative to those of $\bar{D}^0D^0$ has been noted in Refs. [16,17], and [15]. This can be attributed to the much smaller Σ_c^{++}-exchange vertex coupling constant in comparison to that of the Λ_c^+-exchange vertex. However, in the coupled-channels meson-exchange model, the initial-state inelastic interactions could enhance the D^-D^+ cross sections significantly as was discussed earlier. It would be quite interesting to test the predictions of various models for the D^-D^+ cross sections in the $\bar{P}ANDA$ experiment at the upcoming FAIR facility.

As was already noted in Figs. 6(a) and 6(b), the differential cross sections provide more explicit information about the reaction mechanism. These cross sections involve terms that weigh the interference terms of various components of the amplitude with the angles of the outgoing particles. Therefore, in general the contributions of different mechanisms are highlighted in different angular regions. In Fig. 9, we show the predictions of our model for the differential cross sections for the $\bar{p}p \to \bar{D}^0D^0$ reaction at the beam momenta of 8, 10, 12 and 16 GeV/c. In this figure, the solid lines represent cross sections that include the coherent sum of the amplitudes corresponding to the t-channel Λ_c^+ and Σ_c^+ baryon exchanges and the s-channel $\Psi(3770)$ resonance terms, while the dashed lines show the cross sections where the amplitudes include contributions of the Λ_c^+-exchange term only. Since, the Σ_c^+ baryon exchange and the $\Psi(3770)$ resonance contributions are quite small compared to those of the Λ_c^+ exchange, the interference effects of various terms in the amplitudes are not significant at higher beam momenta. We notice that with increasing beam momentum cross sections are more and more forward peaked. This indicates the growing importance of the t-channel exchange terms with increasing beam momenta.

On the other hand, in the differential cross sections of the $\bar{p}p \to D^-D^+$ reaction, the interference effects of the t-channel Σ_c^{++} baryon exchange and the s-channel $\Psi(3770)$ resonance terms are visible even at higher beam momenta, as can be seen in Fig. 10. In this figure the dashed lines represent the cross sections when the contributions of only

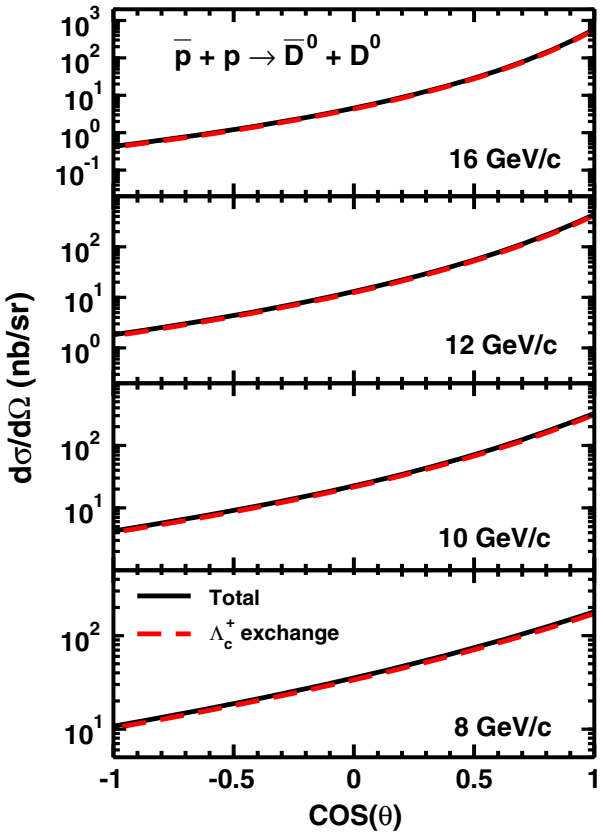

FIG. 9. Differential cross section for the $\bar{p}p \to \bar{D}^0D^0$ reaction at the antiproton beam momenta of 8, 10, 12 and 16 GeV/c as indicated in the figure. The solid lines show the cross sections where the amplitudes of the t-channel Λ_c^+, and Σ_c^+ baryon exchange and s-channel $\Psi(3770)$ resonance terms are coherently added. The dashed lines show the cross sections where the amplitudes include the contributions of the λ_c^+-exchange term only.

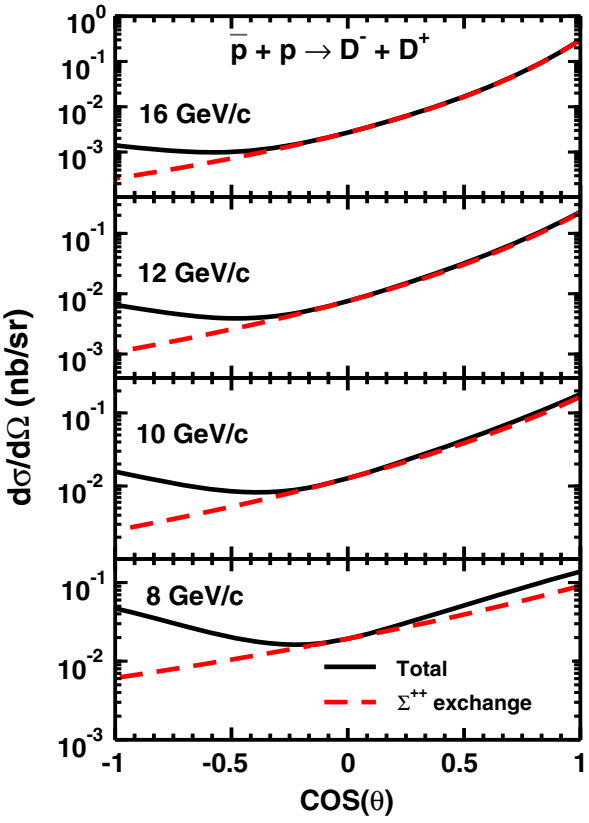

FIG. 10. Differential cross section for the $\bar{p}p \to D^-D^+$ reaction for antiproton beam momenta of 8, 10, 12 and 16 GeV/c. The dashed lines show the contributions of the Σ_c^{++} baryon exchange terms only while the solid line represents the cross sections where the amplitudes of Σ_c^{++} baryon exchange and $\Psi(3770)$ resonance terms are coherently added.

the Σ_c^{++} baryon exchange terms are included in the amplitude, while the solid lines show the results where the amplitudes of Σ_c^{++} baryon exchange and $\Psi(3770)$ resonance terms are coherently added in the cross sections. One notices that the inclusion of the $\Psi(3770)$ resonance terms changes the cross sections drastically at the backward angles. This effect is visible even at the beam momentum of 16 GeV/c. Thus the measurements of the angular distributions of the $\bar{p}p \to D^-D^+$ reaction even at higher beam momenta can provide signals for the $\Psi(3770)$ resonance. Such a study would be complimentary to the methods proposed in Ref. [49].

It should be mentioned here that the physics of the charmed $\bar{D}D$-meson production in $\bar{p}p$ annihilation for beam momenta in excess of 3 GeV may also involve vector resonances other than $\Psi(3770)$. Some of these resonances are J/Ψ, $\Psi(2S)$, $\Psi(4040)$, and $\Psi(4160)$. However, only $\Psi(3770)$ whose mass is just above the $\bar{D}D$ production threshold, has a substantial branching ratio (about 93%) for decay into the $\bar{D}D$ channel [34]. Masses of both J/Ψ and $\Psi(2S)$ are below the $\bar{D}D$ production thresholds and their widths are about 2 orders of magnitude smaller than that of $\Psi(3770)$. Therefore, their decay to the $\bar{D}D$ channel is not possible even from the higher ends of their mass spectrum. Nevertheless, because the mass of $\Psi(2S)$ (3.686 GeV) is just below the $\bar{D}D$ threshold, it may possibly decay to this channel due to of-shell effects. However, no branching ratio is known for this decay mode as per the latest PDG compilation [34]. Therefore, we have not considered this resonance in our work.

On the other hand, the masses of the resonances $\Psi(4040)$ and $\Psi(4160)$ are well above the $\bar{D}D$ threshold, and therefore they can decay to the $\bar{D}D$ channel. However, the branching ratios for these decays are hardly quotable according to the latest PDG compilation. Nevertheless, in Ref. [50] the branching ratios for the decays $\Psi(4040) \to \bar{D}D$ and $\Psi(4160) \to \bar{D}D$ have been estimated by fitting to the $e^+e^- \to \bar{D}D$ data of the Belle Collaboration [51] in the invariant mass region of 3.8–4.3 GeV. In this procedure these resonances are parametrized in terms of the Breit-Wigner form. The estimated branching ratios for the two decay channels are found to be $(25.3 \pm 4.5)\%$ and $(2.8 \pm 1.8)\%$, respectively. These can be used to obtain the coupling constants $g_{\Psi(4040)\bar{D}D}$ and $g_{\Psi(4160)\bar{D}D}$. However, to calculate the cross sections for $\bar{p} + p \to \Psi(4040) \to \bar{D}D$ and $\bar{p} + p \to \Psi(4160) \to \bar{D}D$ processes, we also require the coupling constants $g_{\Psi(4040)\bar{p}p}$ and $g_{\Psi(4160)\bar{p}p}$, about which no information is available. Nevertheless, we performed calculations for the cross sections of these reactions by taking the values of the $g_{\Psi(4040)\bar{p}p}$ and $g_{\Psi(4160)\bar{p}p}$ to be the same as that of $g_{\Psi(3770)\bar{p}p}$. We find that the resulting cross sections in the relevant region are much smaller in comparison to the total cross sections shown in Figs. 7 and 8. Therefore, the inclusion of resonances $\Psi(4040)$ and $\Psi(4160)$ hardly leads to any noticeable change in the overall conclusions of this paper.

Finally, we discuss the uncertainties and the range of the validity of our results. The theoretical approach (the effective Lagrangian model or ELM) considered in this work has mesons and baryons as effective degrees of freedom. This model will be valid in the energy range where consideration of explicit quark degrees of freedom is not required. Therefore, our model is certainly applicable in the range of beam momenta (from threshold to 20 GeV/c) considered in this work. However, the calculations performed within this model are sensitively dependent on the values of the coupling constants at various vertices involved in the t-channel and s-channel diagrams, on the shape of the form factor and the value of the cutoff parameter involved therein, and on the parameters involved in the initial- and final-state interaction scattering matrices. The extents of uncertainty in our results due to all these issues are discussed in the following.

We have taken the coupling constants (CCs) at the vertices involved in the t-channel diagrams from Refs. [31,52,53] where they have been fixed by using the SU(4) symmetry arguments in the description of the exclusive charmed hadron production in the $\bar{D}N$ and DN scattering within a one-boson-exchange picture. The same coupling constants were used in the description of the charmed hadron production within the Jülich meson-exchange model in Refs. [24,40]. Furthermore, these coupling constants were also used in Ref. [30] to investigate the role of intrinsic charm in the nucleon using a phenomenological model formulated in terms of effective meson-baryon degrees of freedom. Thus, the coupling constants used in the calculations of the t-channel diagrams of our model are quite standard. The CCs at the vertices involved in the s-channel diagrams are determined from the experimentally determined branching ratios of the decay of the $\Psi(3770)$ resonance into the relevant channels. Therefore, uncertainties in our cross sections due to the coupling constants are minimal.

There may indeed be some uncertainty in our cross sections coming from the shape of the form factor [and the value of the cutoff parameter (λ_i) involved therein] that are used to regulate the off-shell behavior of various vertices. As stated above, we have employed a monopole form factor as given by Eq. (3), with a λ_i of 3.0 GeV. A form factor of a different shape and/or a different value of the cutoff parameter would lead to a different cross section. For example, using a quadrupole form factor [of the type given by Eq. (4)] with the same cutoff parameter leads to enhancement in the cross sections by factors of 3–4. Changing λ_i from 3 to 3.5 increases the cross sections by a factor of up to 2. We have tried to minimize these uncertainties in the cross sections by using the same shape (monopole) of the form factor and the same value of λ_i that were used in our previous study of the charmed baryon

production [29]. As in other cases, issues related to the form factor will be finally settled once the data become available on the charmed meson and baryon production in $\bar{p}p$ annihilation from the $\bar{P}ANDA$ experiment.

The initial- and final-state interactions, which are the important ingredients of our model, provide another source of uncertainty in our results. We treat these effects within an eikonal-approximation-based phenomenological method. Generally, the parameters of this model are constrained by fitting to the experimental data. Because of the lack of any experimental information, it is not yet possible to test our model thoroughly. The absolute magnitude of our cross sections may have some uncertainties due to this. Nevertheless, in our study we have used the same set of distortion parameters that were used in our previous calculations of the charmed baryon production in the same reaction. These parameters reproduce the data for the $\bar{\Lambda}\Lambda$ channel and the cross sections for the $\bar{\Lambda}_c\Lambda_c$ channel calculated within the Jülich meson-exchange model where distortion effects are treated more rigorously within a coupled-channels approach. Therefore, the initial and final channel distortion effects included in our model are checked against the other independent sources.

IV. SUMMARY AND CONCLUSIONS

In summary, we studied the $\bar{p}+p\to\bar{D}^0D^0$ and $\bar{p}+p\to D^-D^+$ reactions by using a single-channel effective Lagrangian model that involves the meson-baryon degrees of freedom. The dynamics of the production process has been described by the t-channel Λ_c^+, Σ_c^+ and Σ_c^{++} baryon exchange diagrams and also the s-channel excitation, propagation and decay of the $\Psi(3770)$ resonance. The initial- and final-state interactions have been accounted for by an eikonal type of phenomenological model. The coupling constants at the baryon exchange vertices were taken from Refs. [31,52,53], which were the same as those used in the study of the $\bar{p}+p\to\bar{\Lambda}_c^-\Lambda_c^+$ reaction at the similar vertices in Ref. [29]. The CCs at $\Psi\bar{p}p$, $\Psi\bar{D}^0D^0$ and ΨD^-D^+ vertices have been determined from the branching ratios for the decay of the $\Psi(3770)$ resonance into the relevant channels as given in Refs. [35] and [36]. The off-shell corrections at various vertices have been accounted for by introducing monopole form factors with a cutoff parameter of 3.0 GeV. The same form factor with the same value of the cutoff parameter was also used in our study of the $\bar{p}+p\to\bar{\Lambda}_c^-\Lambda_c^+$ reaction [29]. The parameters involved in the initial-state interaction scattering matrices were also taken to be the same as those used in Ref. [29].

Since the cross sections of the $\bar{p}+p\to D^-D^+$ reaction are strongly suppressed due to the smaller coupling constants of the vertices involving Σ_c^{++} baryon exchange, the inclusion of the $\Psi(3770)$ resonance produces a sizable enhancement in the $\bar{p}+p\to D^-D^+$ cross sections around the resonance energy. However, their effect is not so strong in case of the $\bar{p}+p\to\bar{D}^0D^0$ reaction where the baryon exchange cross sections are quite large—they vary between 100–400 nb for antiproton beam momenta between 6.4–6.8 GeV/c. Therefore, the inclusion of the $\Psi(3770)$ resonance in this case produces only a small kink in the total cross section near the resonance energy.

On the other hand, the differential cross sections for both the reactions are affected in a major way by the $\Psi(3770)$ resonance contributions for antiproton beam momentum near the resonance peak. In case of the $\bar{p}+p\to\bar{D}^0D^0$ reaction, the Ψ resonance contributions introduce a sizable reduction (enhancement) in the DCS at the backward (forward) angles. For the $\bar{p}+p\to D^-D^+$ reaction, the shape of the DCS changes drastically by the inclusion of the Ψ resonance term—it changes to a p-wave type of distribution from a s-wave shape. This drastic shape change of the DCS can perhaps be exploited in a dedicated experiment at the $\bar{P}ANDA$ facility to pin down the $\Psi(3770)$ resonance.

At higher antiproton momenta, the total cross section of the $\bar{p}+p\to\bar{D}^0D^0$ reaction is dominated by the contributions of the Λ_c^+ baryon exchange. The cross section peaks around a $p_{\bar{p}}^{\rm lab}$ of 9 GeV/c. At a $p_{\bar{p}}^{\rm lab}$ of 15 GeV/c, which is of interest to the $\bar{P}ANDA$ experiment, the total cross section of this reaction is about 550 nb which is at least 5 times larger than the largest value of this cross section reported previously. Of course, previous calculations have used different types of models that invoke explicitly the quark degrees of freedom in their calculations, which may make them more adequate for energies higher than those of the $\bar{P}ANDA$ experiment. Therefore, it is not trivial to understand the reasons for the large difference seen between their cross section and ours. The future $\bar{P}ANDA$ experiments at FAIR are expected to clarify the situation.

Within our model the cross sections of the $\bar{p}+p\to D^-D^+$ reaction are strongly suppressed as compared to those of the $\bar{p}+p\to\bar{D}^0D^0$ reaction. This is due to the fact that the latter is dominated by the Λ_c^+ baryon exchange mechanism, while the former gets a contribution only from the Σ_c^{++} exchange whose couplings are much lower than those of the Λ_c^+ exchange vertices. However, in the coupled-channels meson-exchange model of Ref. [21], the $\bar{p}+p\to D^-D^+$ cross sections are even larger than the $\bar{p}+p\to\bar{D}^0D^0$ ones. This is a result of the coupled-channels treatment in the incident channel which accounts effectively for two-step inelastic processes involving Λ_c^+ "baryon exchange."

The differential cross sections of the $\bar{p}+p\to\bar{D}^0D^0$ reaction at higher values of $p_{\bar{p}}^{\rm lab}$ are strongly forward peaked and are so strongly dominated by the contributions of the Λ_c^+ baryon exchange terms that the interference terms of various other contributions (Σ_c^+ baryon exchange and Ψ resonance) become insignificant. However, in the case of the $\bar{p}+p\to D^-D^+$ reaction, differential cross sections

have significant contributions from the interference terms of Σ_c^{++} baryon exchange and the Ψ resonance process even at higher antiproton beam momenta. In view of these results, it should be possible to pin down the $\Psi(3770)$ resonance contributions in these reactions in dedicated experiments in the relevant antiproton energy regions.

ACKNOWLEDGMENTS

This work has been supported by the Deutsche Forschungsgemeinschaft (DFG) under Grant No. Le439/8-2 and the Helmholtz International Center (HIC) for FAIR and the Council of Scientific and Industrial Research (CSIR), India.

[1] J. Aubert *et al.*, Phys. Rev. Lett. **33**, 1404 (1974).
[2] J. Augustin *et al.*, Phys. Rev. Lett. **33**, 1406 (1974).
[3] G. T. Bodwin, arXiv:1208.5506, Report ANL-HEP-CP-12-64.
[4] T. Kawanai and S. Sasaki, arXiv:1503.05752.
[5] S. Prelovsek, *Proc. Sci.*, LATTICE2014 (2014) 015, arXiv:1411.0405.
[6] W. Erni *et al.*, arXiv:0903.3905.
[7] U. Wiedner, Prog. Part. Nucl. Phys. **66**, 477 (2011).
[8] E. Prencipe, Eur. Phys. J. Web Conf. **95**, 04052 (2015).
[9] C. B. Dover and S. H. Kahana, Phys. Rev. Lett. **39**, 1506 (1977).
[10] K. Tsushima and F. C. Khanna, Phys. Rev. C **67**, 015211 (2003).
[11] K. Tsushima and F. C. Khanna, J. Phys. G **30**, 1765 (2004).
[12] K. Tsushima, D. H. Lu, A. W. Thomas, K. Saito, and R. H. Landau, Phys. Rev. C **59**, 2824 (1999).
[13] C. Garcia-Recio, J. Nieves, and L. Tolos, Phys. Lett. B **690**, 369 (2010).
[14] C. Garcia-Recio, J. Nieves, L. L. Salcedo, and L. Tolos, Phys. Rev. C **85**, 025203 (2012).
[15] A. B. Kaidalov and P. E. Volkovitsky, Z. Phys. C **63**, 517 (1994).
[16] A. Khodjamirian, C. Klein, T. Mannel, and Y.-M. Wang, Eur. Phys. J. A **48**, 31 (2012).
[17] A. I. Titov and B. Kämpfer, Phys. Rev. C **78**, 025201 (2008).
[18] A. T. Goritschnig, B. Pire, and W. Schweiger, Phys. Rev. D **87**, 014017 (2013); **88**, 079903(E) (2013).
[19] A. T. Goritschnig, P. Kroll, and W. Schweiger, Eur. Phys. J. A **42**, 43 (2009).
[20] P. Kroll, B. Quadder, and W. Schweiger, Nucl. Phys. **B316**, 373 (1989).
[21] J. Haidenbauer and G. Krein, Phys. Rev. D **89**, 114003 (2014).
[22] J. Haidenbauer, T. Hippchen, K. Holinde, B. Holzenkamp, V. Mull, and J. Speth, Phys. Rev. C **45**, 931 (1992).
[23] J. Haidenbauer, K. Holinde, V. Mull, and J. Speth, Phys. Rev. C **46**, 2158 (1992).
[24] J. Haidenbauer and G. Krein, Phys. Lett. B **687**, 314 (2010).
[25] J. Haidenbauer and G. Krein, Few-Body Syst. **50**, 183 (2011).
[26] R. Shyam, Phys. Rev. C **60**, 055213 (1999).
[27] R. Shyam and U. Mosel, Phys. Rev. C **67**, 065202 (2003).
[28] R. Shyam, O. Scholten, and A. W. Thomas, Phys. Rev. C **84**, 042201(R) (2011).
[29] R. Shyam and H. Lenske, Phys. Rev. D **90**, 014017 (2014).
[30] T. J. Hobbs, J. T. Londergan, and W. Melnitchouk, Phys. Rev. D **89**, 074008 (2014).
[31] J. Haidenbauer, G. Krein, U.-G. Meissner, and L. Tolos, Eur. Phys. J. A **47**, 18 (2011).
[32] A. Müller-Groeling, K. Holinde, and J. Speth, Nucl. Phys. **A513**, 557 (1990).
[33] J. Van de Wiele and S. Ong, Eur. Phys. J. A **46**, 291 (2010).
[34] K. A. Olive (Particle Data Group), Chin. Phys. C **38**, 090001 (2014).
[35] M. Ablikim *et al.* (BES Collaboration), Phys. Rev. Lett. **97**, 121801 (2006).
[36] M. Ablikim *et al.* (BESIII Collaboration), Phys. Lett. B **735**, 101 (2014).
[37] G.-Y. Chen and Q. Zhao, Phys. Lett. B **718**, 1369 (2013).
[38] Y.-J. Zhang and Q. Zhao, Phys. Rev. D **81**, 034011 (2010).
[39] A. Limphirat, W. Sreethawong, K. Khosonthongkee, and Y. Yan, Phys. Rev. D **89**, 054030 (2014).
[40] J. Haidenbauer and G. Krein, Phys. Rev. D **91**, 114022 (2015).
[41] S. Teis, W. Cassing, M. Effenberger, A. Hombach, U. Mosel, and Gy. Wolf, Z. Phys. A **356**, 421 (1997).
[42] N. N. Achasov and G. N. Shestakov, Phys. Rev. D **86**, 114013 (2012).
[43] J. M. Blatt and V. F. Weisskopf, *Theoretical Nuclear Physics* (Wiley, New York, 1952).
[44] M. Kohono and W. Weise, Nucl. Phys. **A454**, 429 (1986).
[45] M. A. Alberg, E. M. Henley, L. Wilets, and P. D. Kunz, Nucl. Phys. **A560**, 365 (1993).
[46] N. J. Sopkovich, Nuovo Cimento **26**, 186 (1962).
[47] W. Roberts, Z. Phys. C **49**, 633 (1991).
[48] D. Lohse, J. W. Durso, K. Holinde, and J. Speth, Nucl. Phys. **A516**, 513 (1990).
[49] C. W. Xiao and E. Oset, Eur. Phys. J. A **49**, 52 (2013).
[50] H.-B. Li, X.-S. Qin, and M.-Z. Yang, Phys. Rev. D **81**, 011501(R) (2010).
[51] G. Pakhlova *et al.* (Belle Collaboration), Phys. Rev. D **77**, 011103(R) (2008).
[52] J. Haidenbauer, G. Krein, U.-G. Meissner, and A. Sibirtsev, Eur. Phys. J. A **33**, 107 (2007).
[53] J. Haidenbauer, G. Krein, U.-G. Meissner, and A. Sibirtsev, Eur. Phys. J. A **37**, 55 (2008).